Supplementary Information (SI) for CrystEngComm.
This journal is © The Royal Society of Chemistry 2025

Supplementary Materials

Coordination Polymers Constructed from Bis-pyridyl-bis-amide and 1,4,5,8-Naphthalenetetracarboxylic Acid: Ligand Transformation and Metal Sensing

Wei-Hao Chen,[1] Yan-Xin Chen,[1] Kedar Bahadur Thapa,[2] Shih-Miao Liu[3]* and Jhy-Der Chen[1]*

[1]*Department of Chemistry, Chung Yuan Christian University, Chung-Li, Taiwan, R.O.C. E-mail: jdchen@cycu.edu.tw*

[2]*Makawanpur Multiple Campus, affiliated to Tribhuvan University, Municipality Rd, Hetauda, Nepal*

[3]*Center for General Education, Hsin Sheng Junior College of Medical Care and Management, Longtan, Taiwan, R.O.C. E-mail: lsm0301@hsc.edu.tw*

Fig. S1. PXRD patterns of complex **1**.

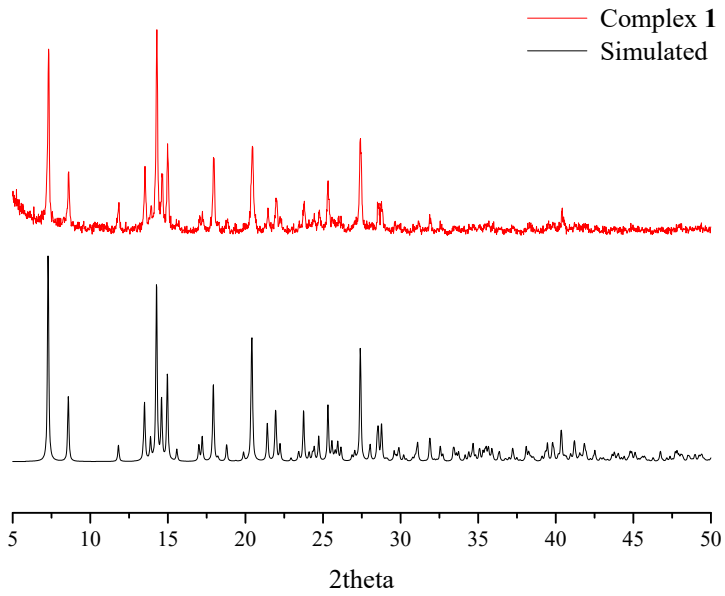

Fig. S2. PXRD patterns of complex **2**.

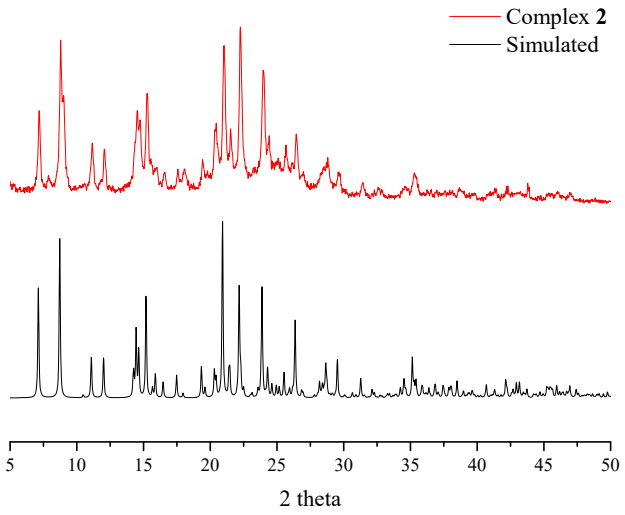

Fig. S3. PXRD patterns of complex **3**.

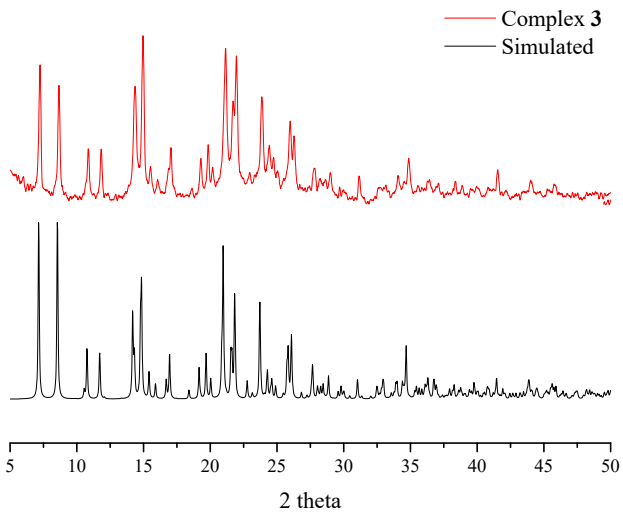

Fig. S4. PXRD patterns of complex **4**.

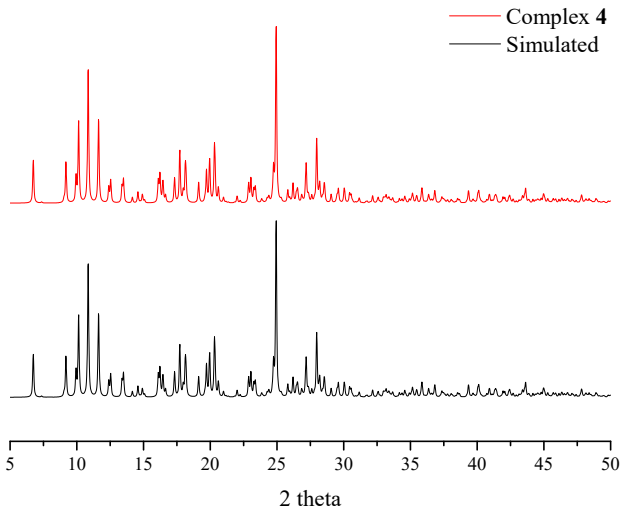

Fig. S5. PXRD patterns of complex **5a**.

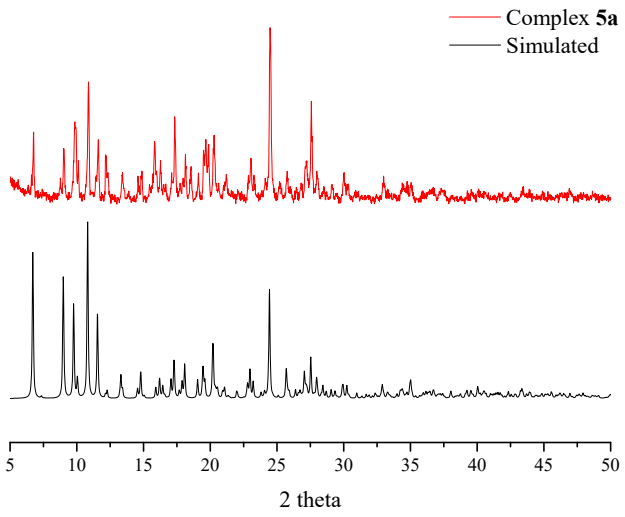

Fig. S6. PXRD patterns of complex **5b**.

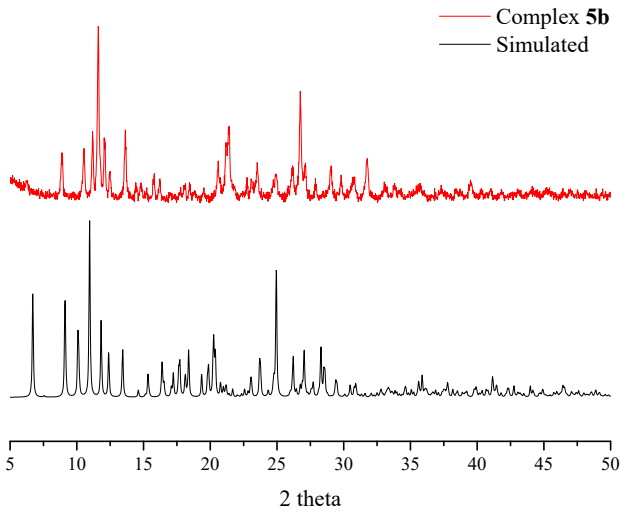

Fig. S7. PXRD patterns of complex **6**.

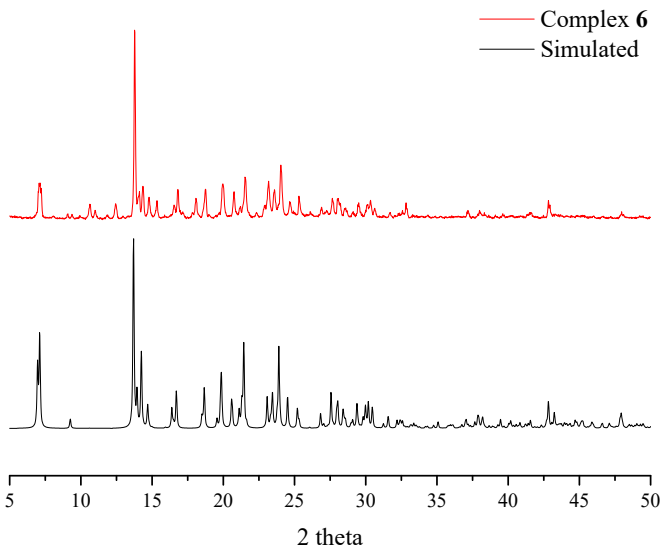

Fig. S8. PXRD patterns of complex **7**.

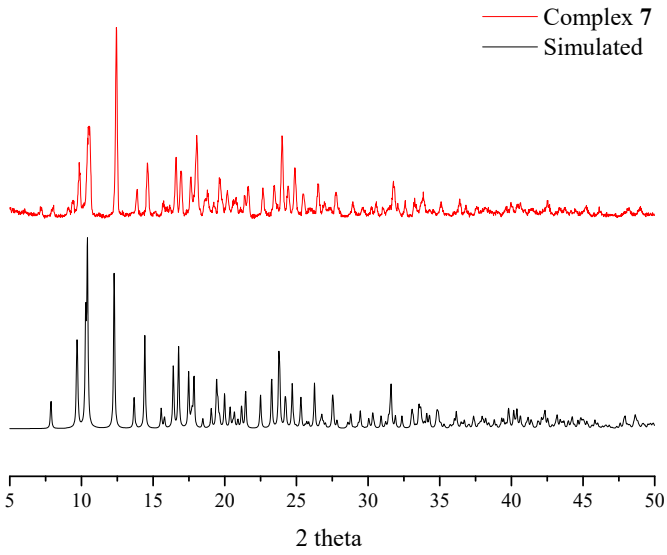

Fig. S9. TGA curve of complex **1**.

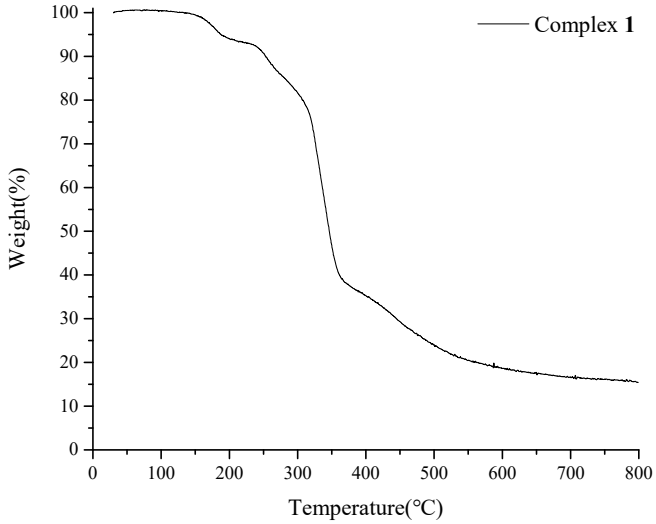

Fig. S10. TGA curve of complex **2**.

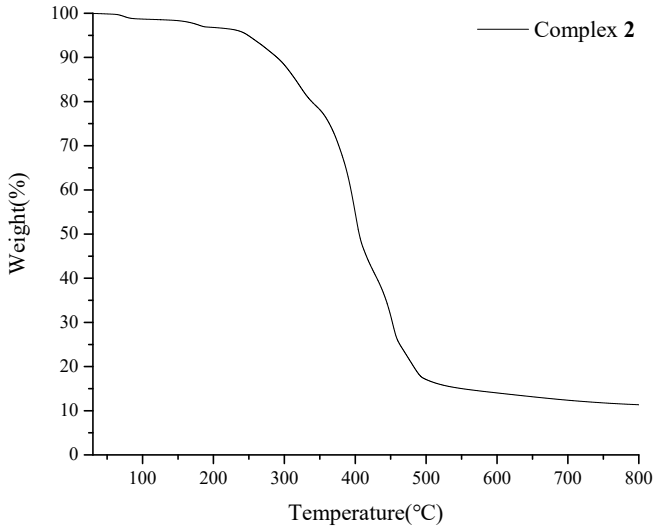

Fig. S11. TGA curve of complex **3**.

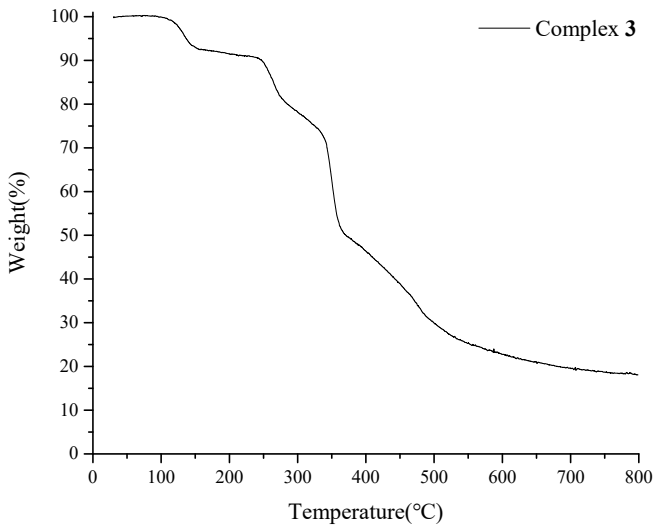

Fig. S12. TGA curve of complex **4**.

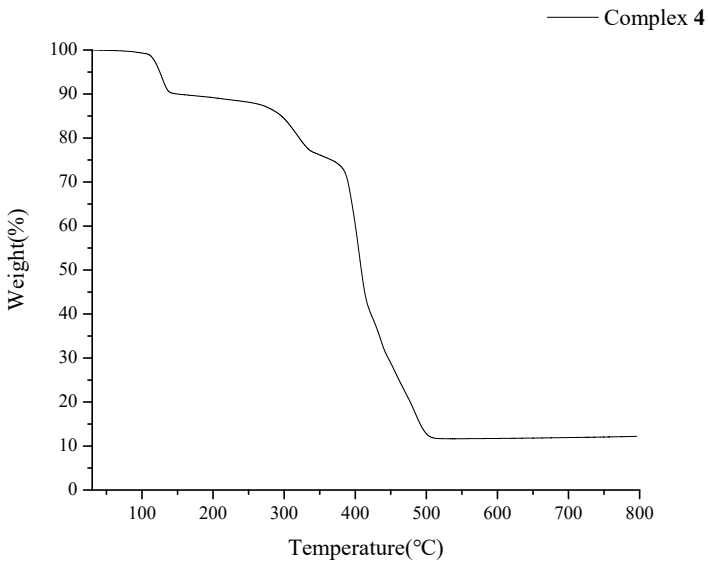

Fig. S13. TGA curve of complex **5a**.

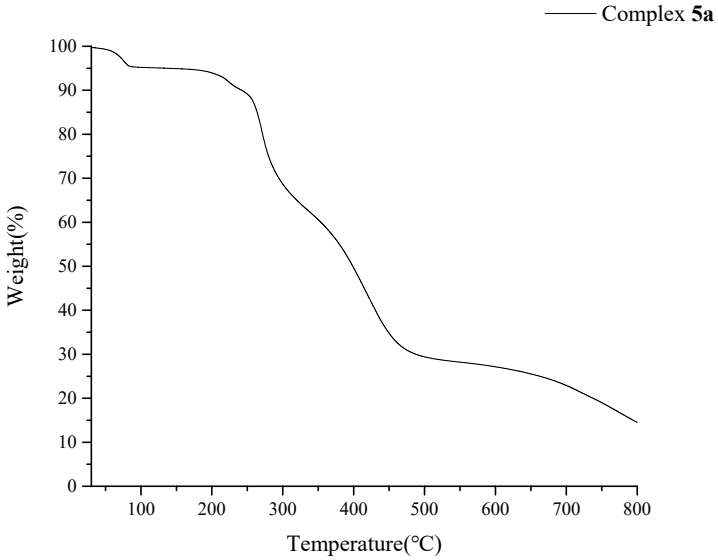

Fig. S14. TGA curve of complex **5b**.

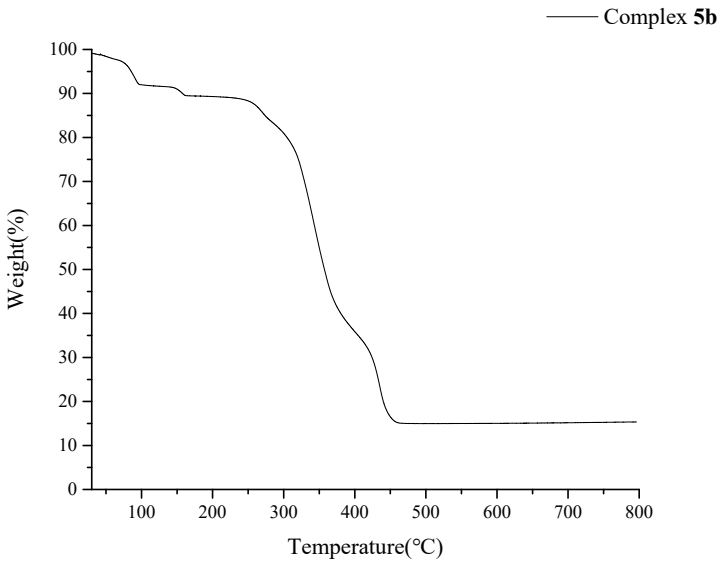

Fig. S15. TGA curve of complex **6**.

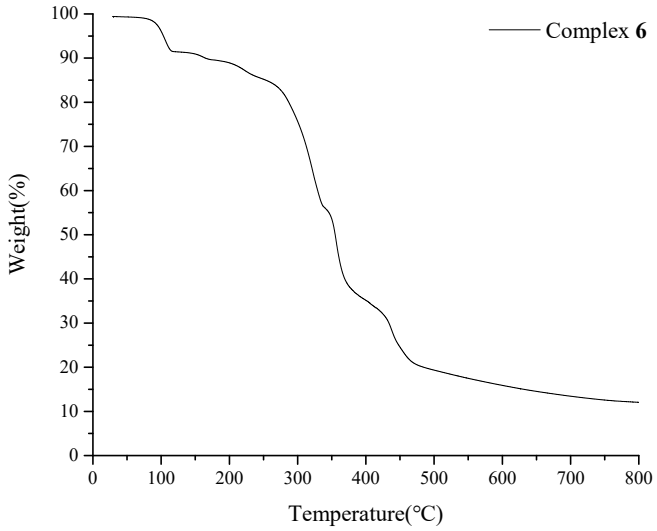

Fig. S16. TGA curve of complex **7**.

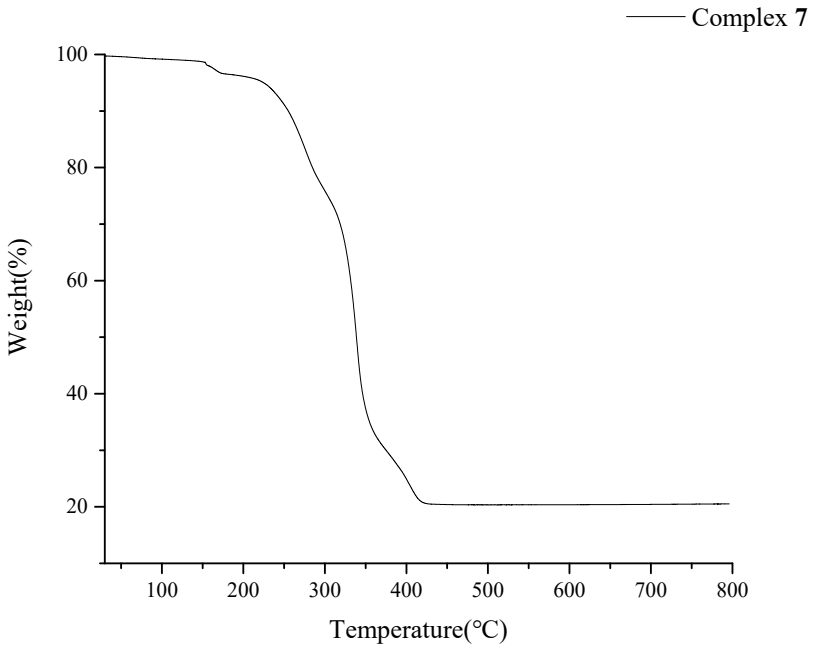

Fig. S17. PXRD patterns of complex **1** in different solvents

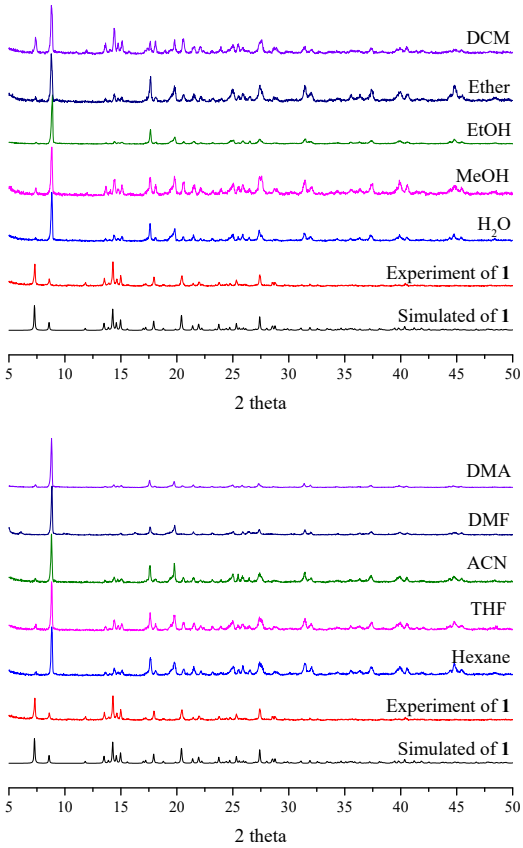

Fig. S18. PXRD patterns of complex **2** in different solvents

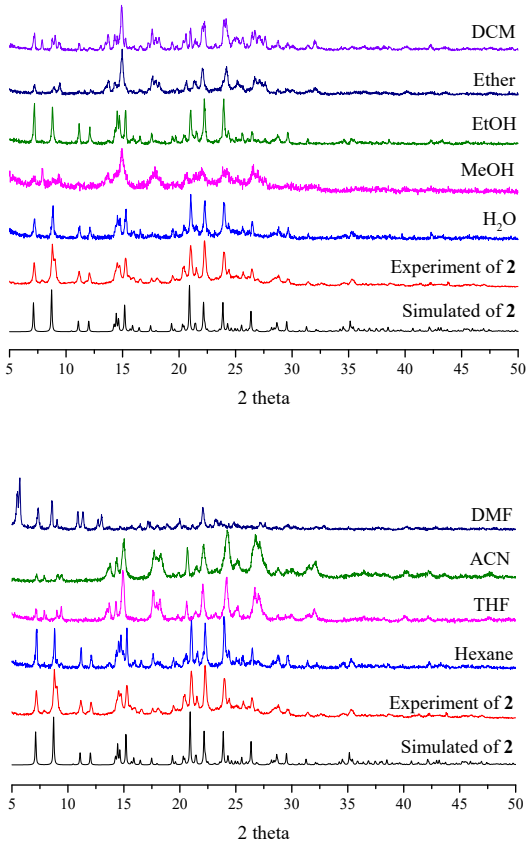

Fig. S19. PXRD patterns of complex **3** in different solvents

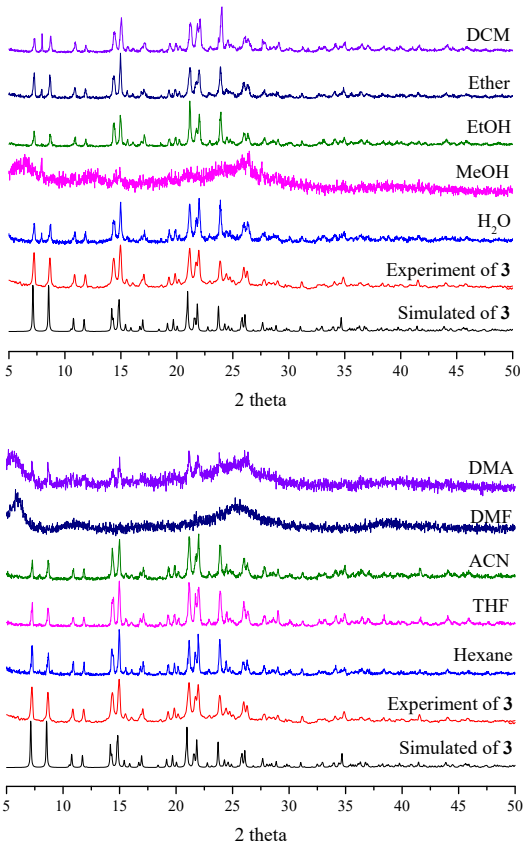

Fig. S20. PXRD patterns of complex **6** in different solvents

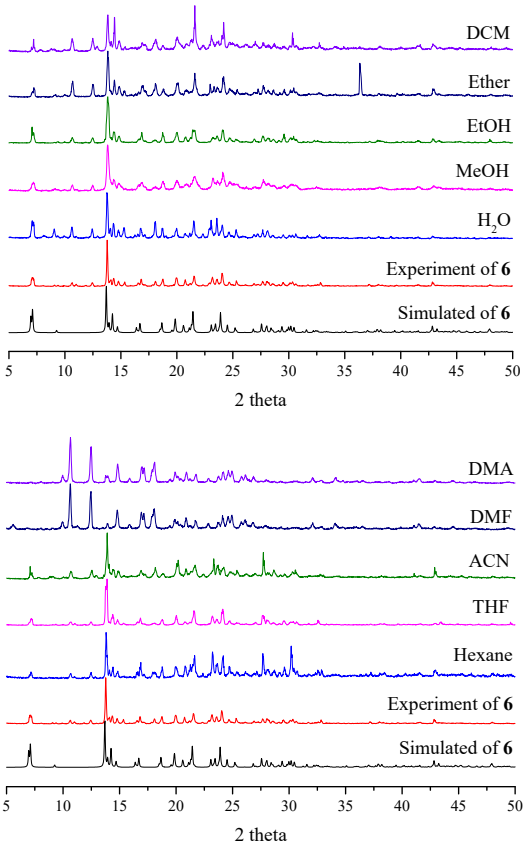

Fig. S21. PXRD patterns of complex **7** in different solvents

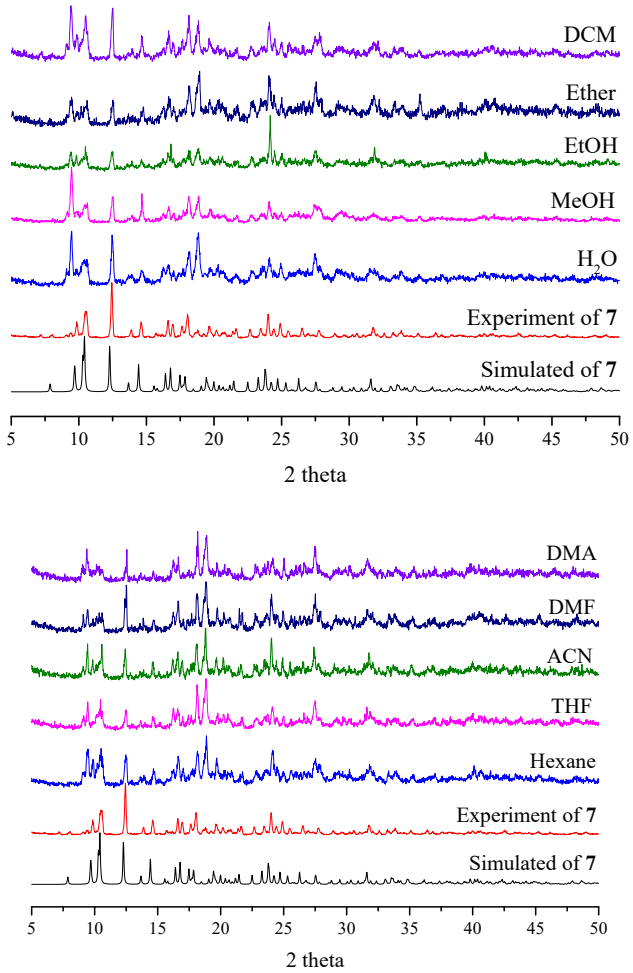

Fig. S22. The emission and excitation spectra of $\mathbf{L^1}$ and $\mathbf{L^2}$.

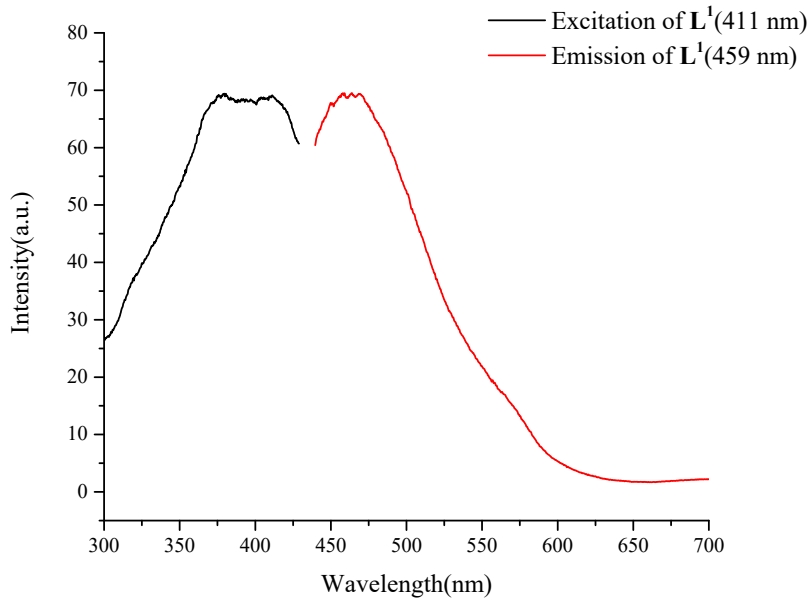

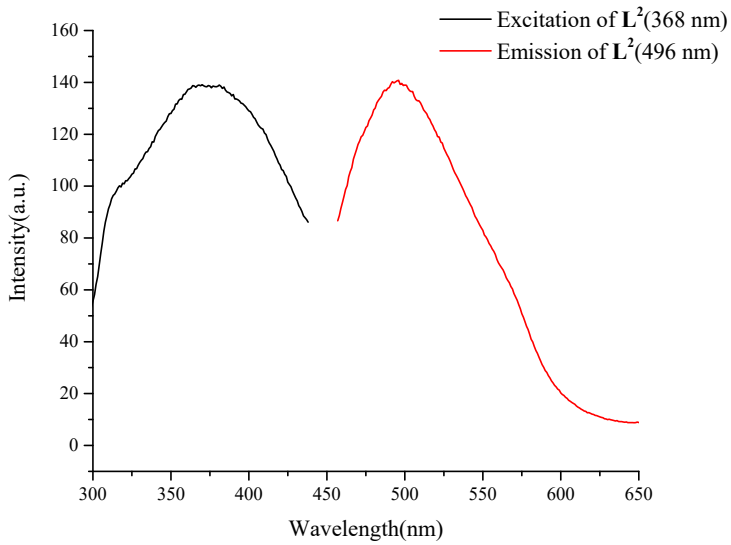

Fig. S23. The emission and excitation spectra of $\mathbf{L^4}$ and H_4NTC.

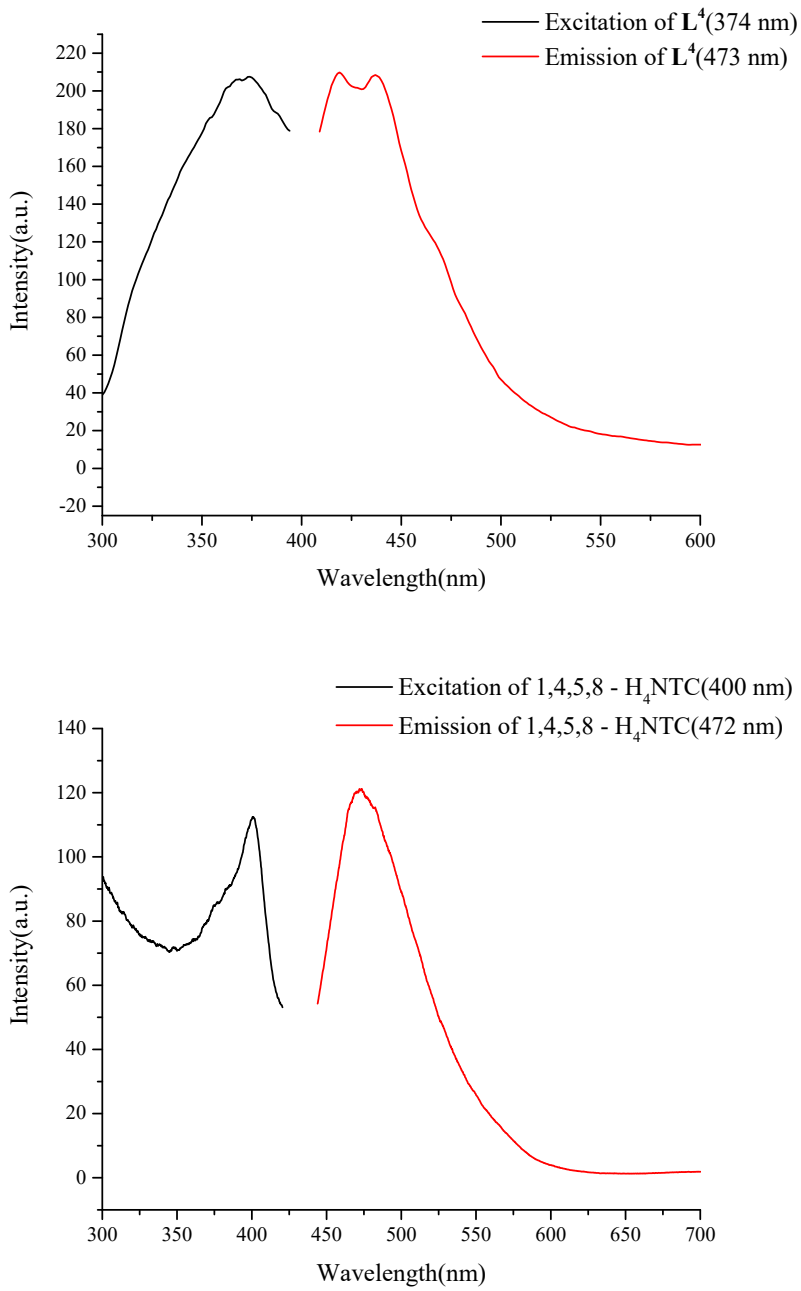

Fig. S24. The emission and excitation spectra of complexes **1** and **2**.

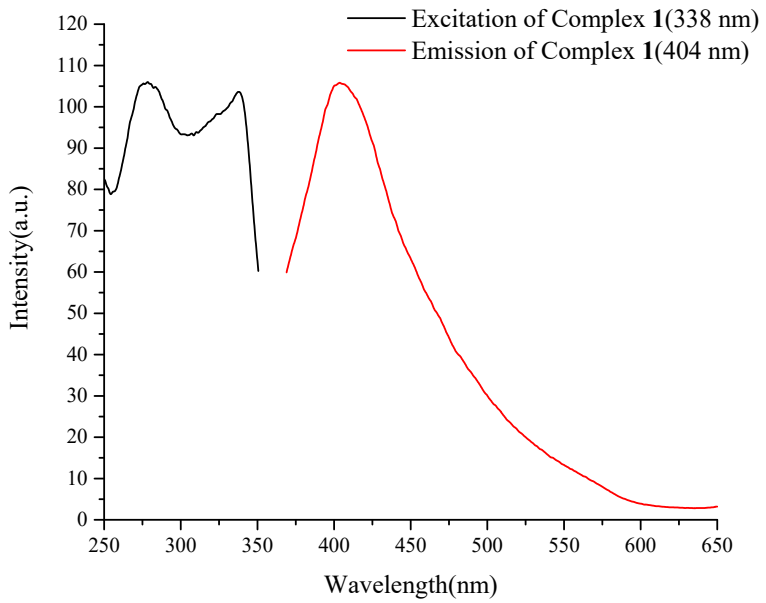

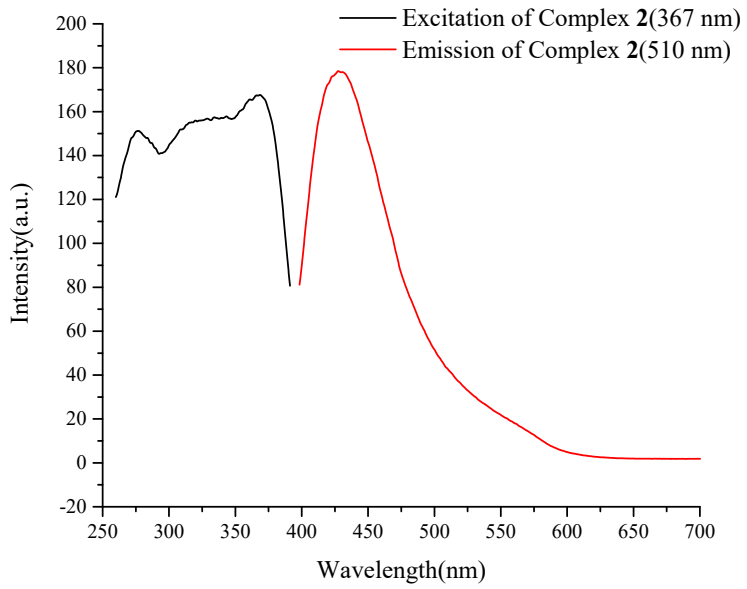

Fig. S25. The emission and excitation spectra of complexes **3** and **6**.

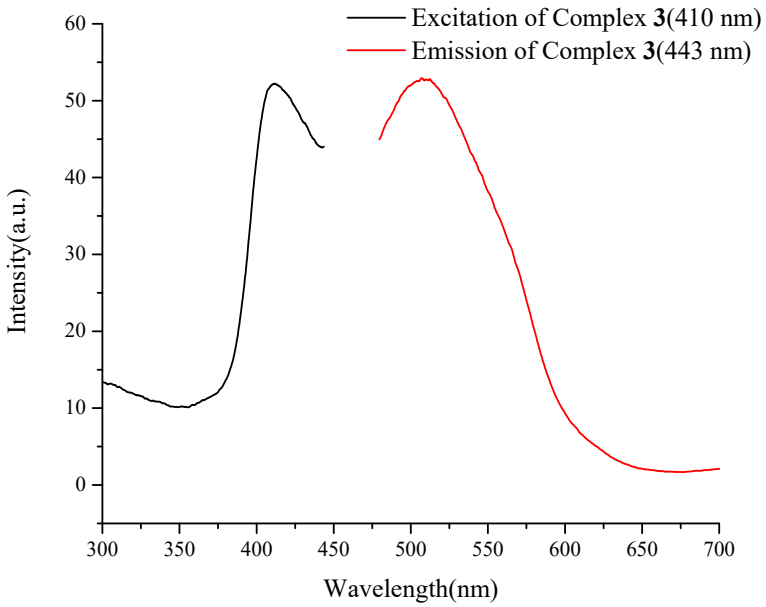

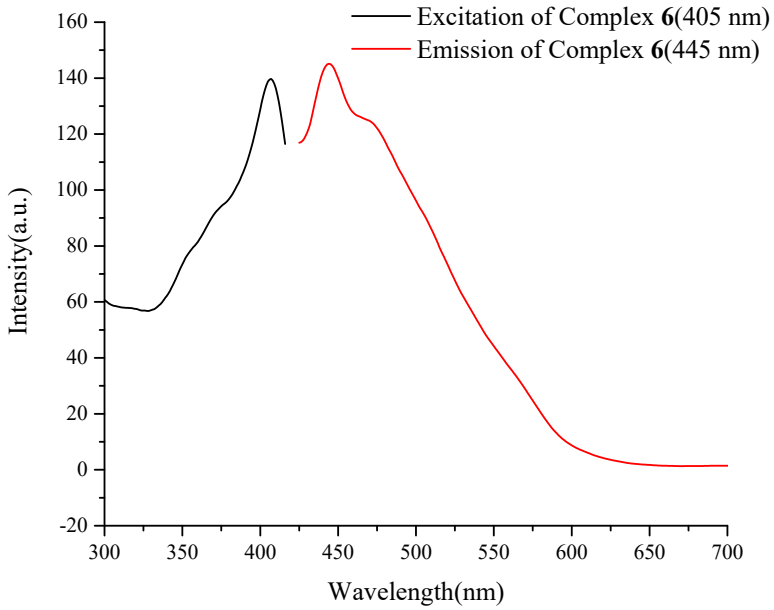

Fig. S26. The emission and excitation spectra of complex **7**.

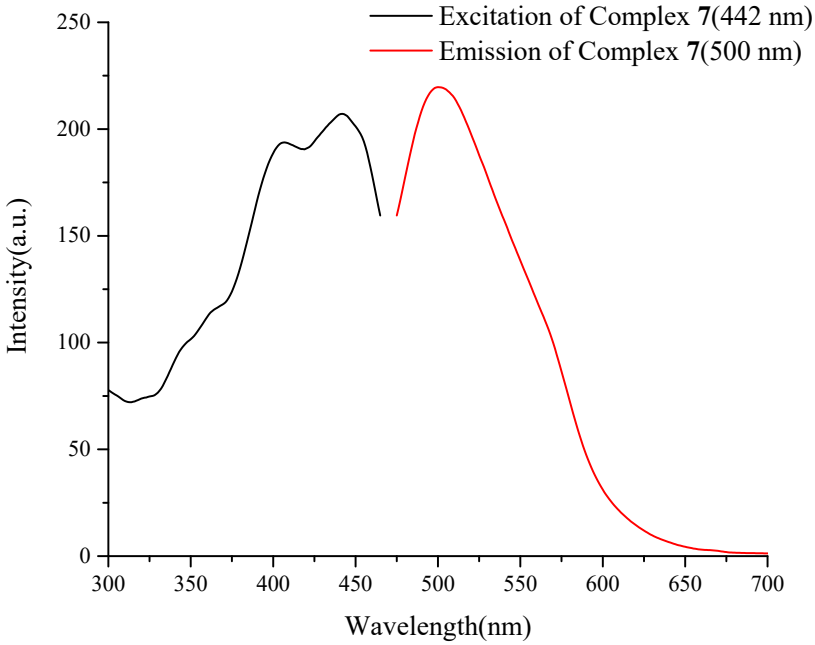

Fig. S27. Emission spectra and the bar charts showing the percentages of quenching of complex **1** for triplicate experiments.

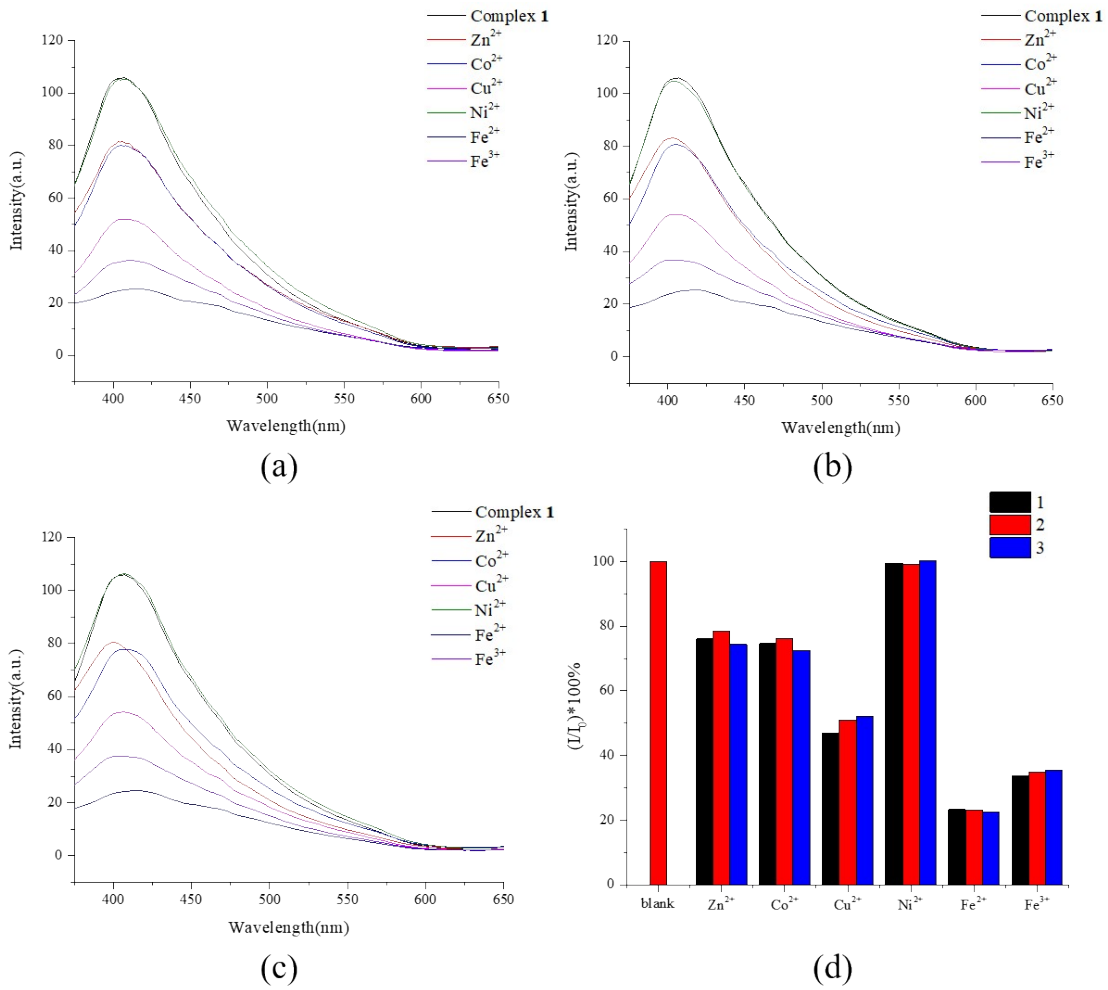

Fig. S28. Emission spectra and the bar charts showing the percentages of quenching of complex **2** for triplicate experiments.

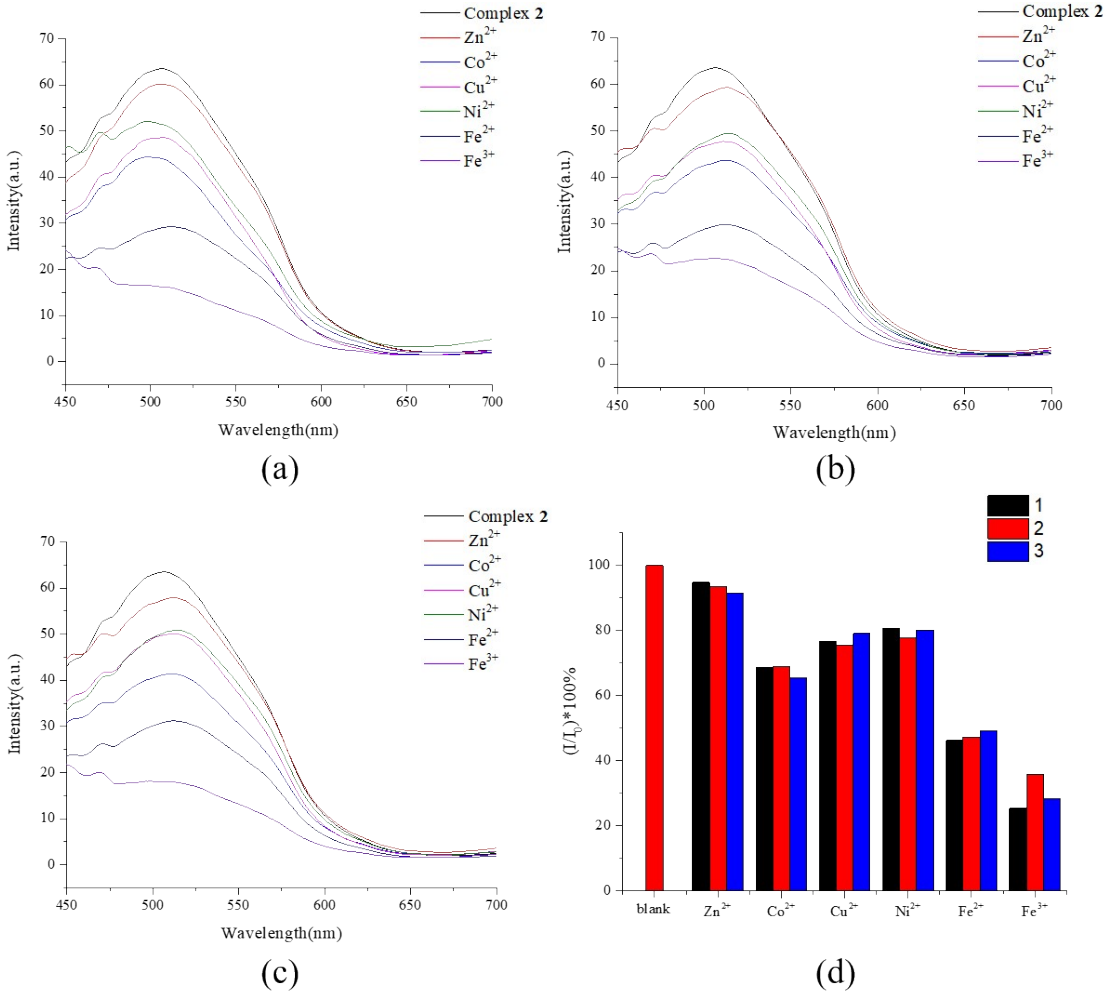

Fig. S29. Emission spectra and the bar charts showing the percentages of quenching of complex **3** for triplicate experiments.

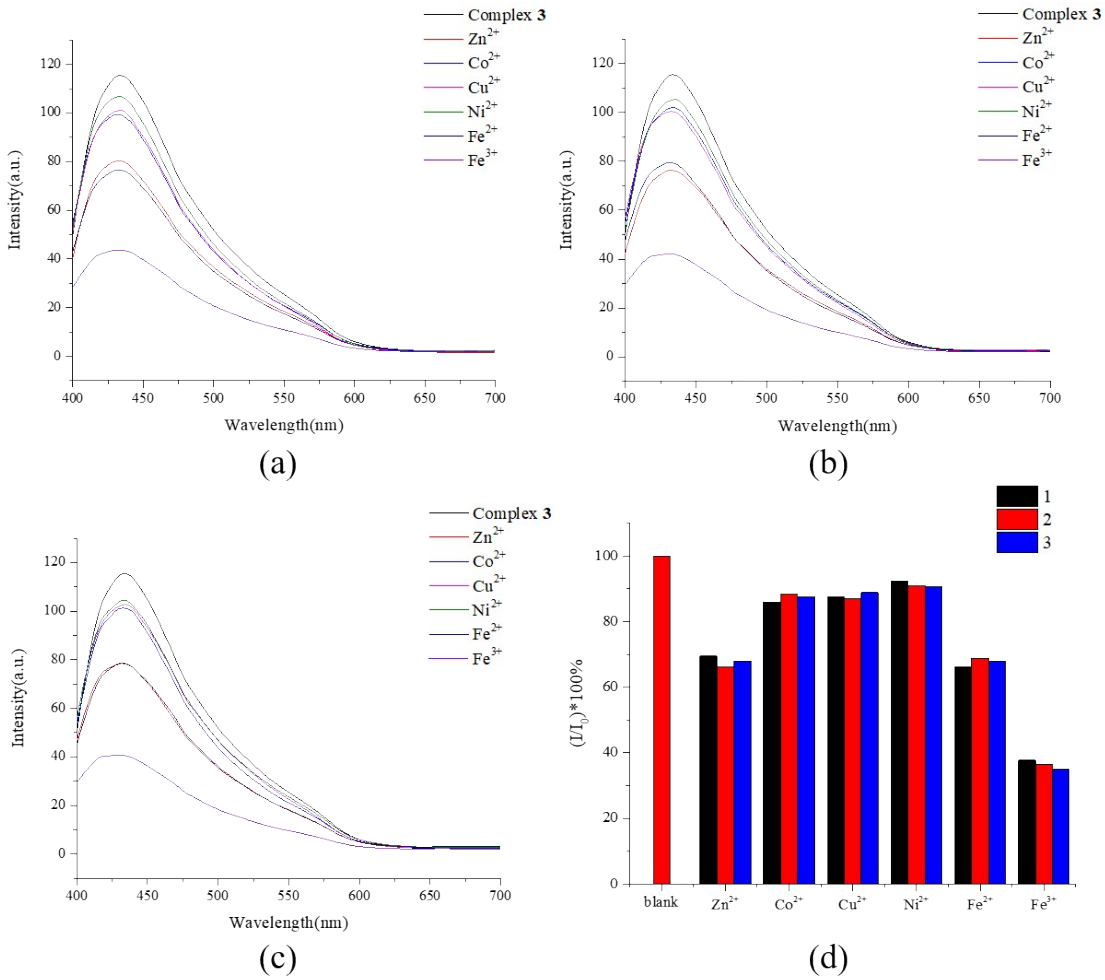

Fig. S30. Emission spectra and the bar charts showing the percentages of quenching of complex **6** for triplicate experiments.

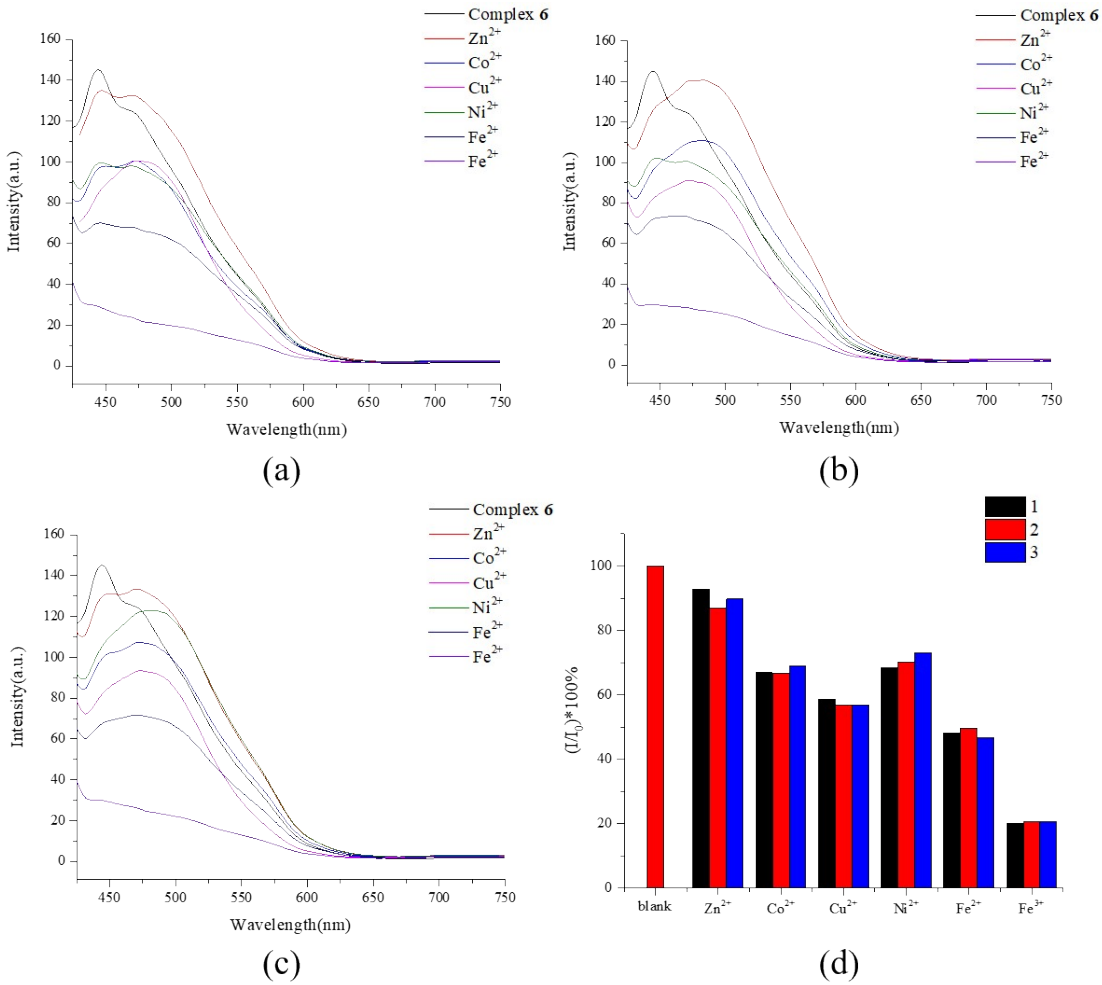

Fig. S31. Emission spectra and the bar charts showing the percentages of quenching of complex **7** for triplicate experiments.

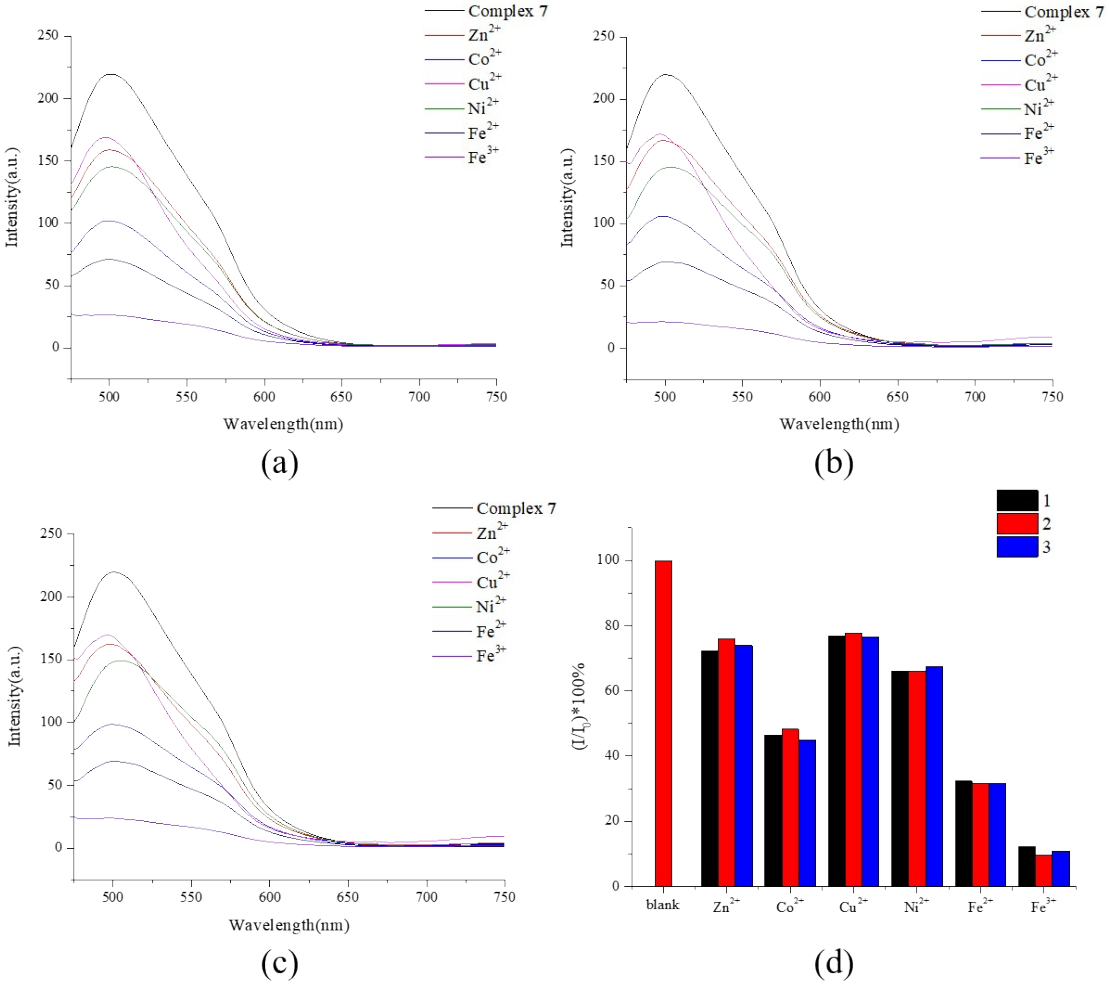

Fig. S32. PXRD patterns of complex **7** in different cationic solutions.

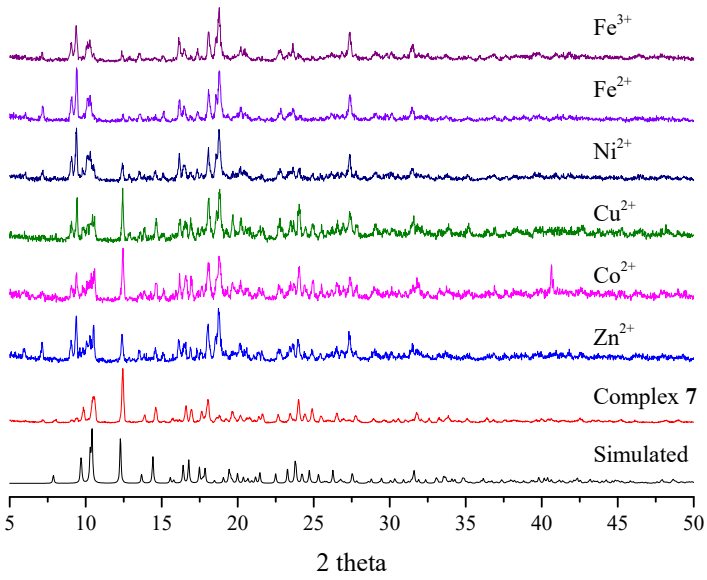

Fig. S33. A drawing showing the overlap of the excitation spectrum of complex **7** and the UV-vis spectrum of Fe^{3+}.

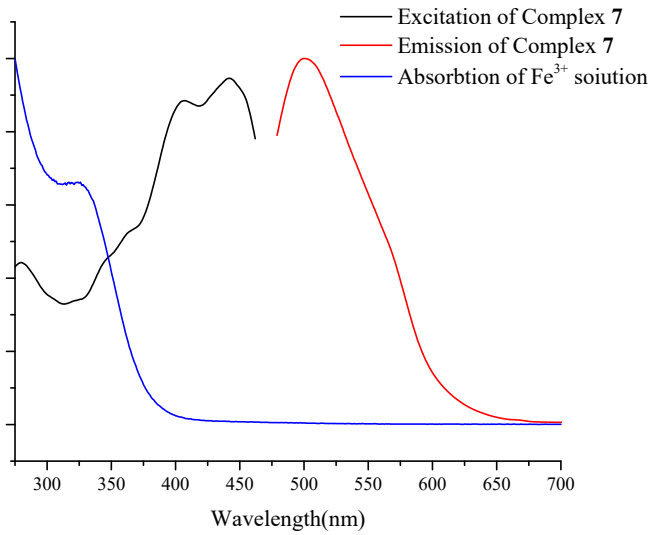

Fig. S34. The EDX data of complex **7** in Fe^{3+}.

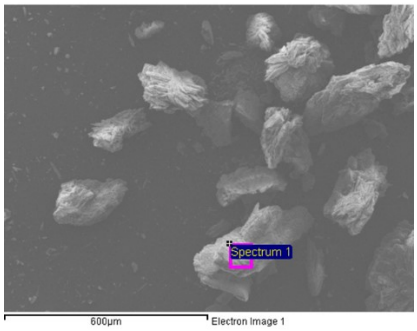

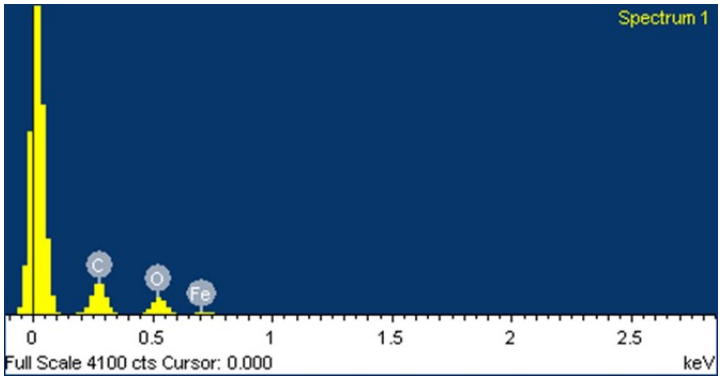

The element percentage analysis of point scan.

Element	Weight%	Atomic%
C K	43.13	60.46
O K	31.57	33.23
Fe L	16.60	5.00
Cd L	8.70	1.30
Totals	100.00	100.00

Fig. S35. IR spectra of complex **7** before and after immersion in Fe^{3+}.

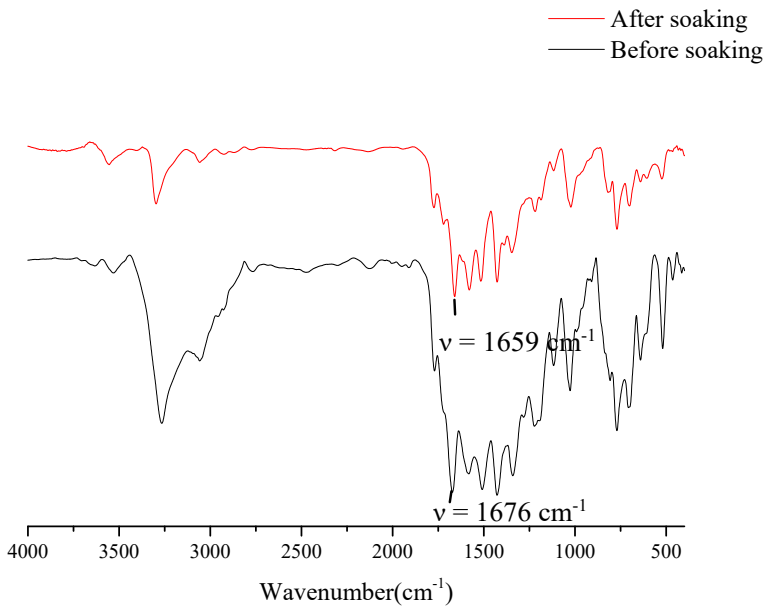

Fig. S36. Full XPS spectra of complex **7**.

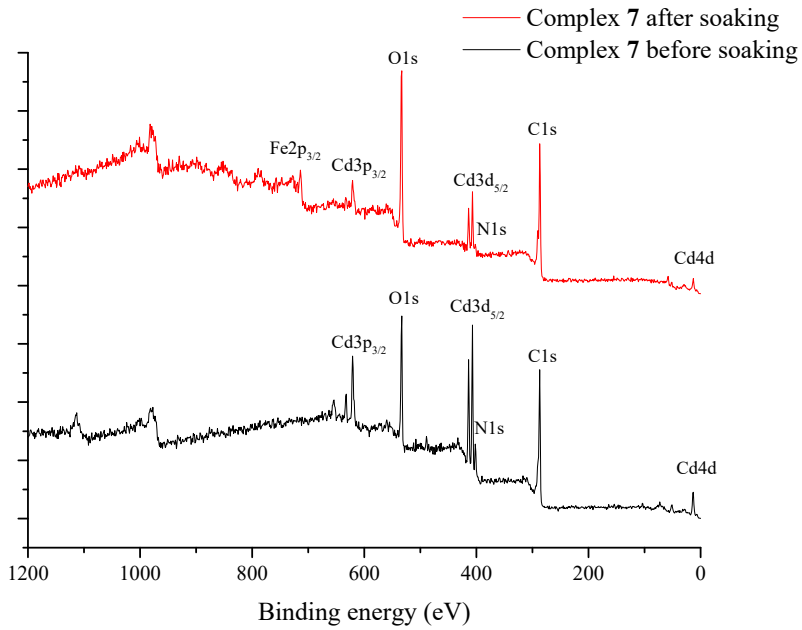

Fig. S37. Binding energies fitting analysis for O1s electrons of complex **7** (a) before and (b) after immersing in Fe^{3+}.

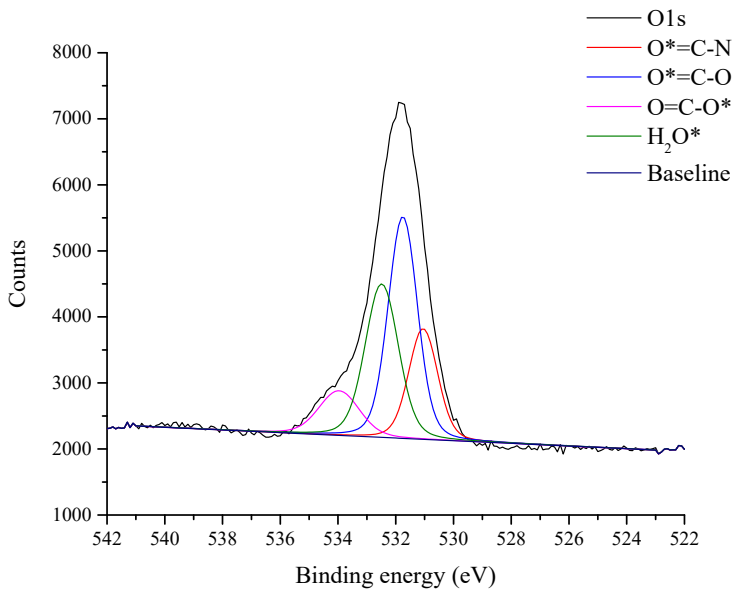

(a)

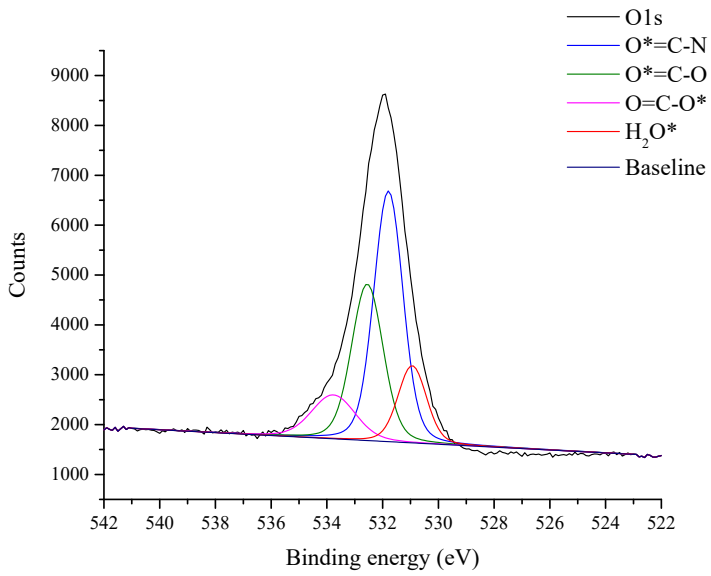

(b)

Fig. S38. The emission spectra of complex **7** in Fe^{3+} with different concentrations.

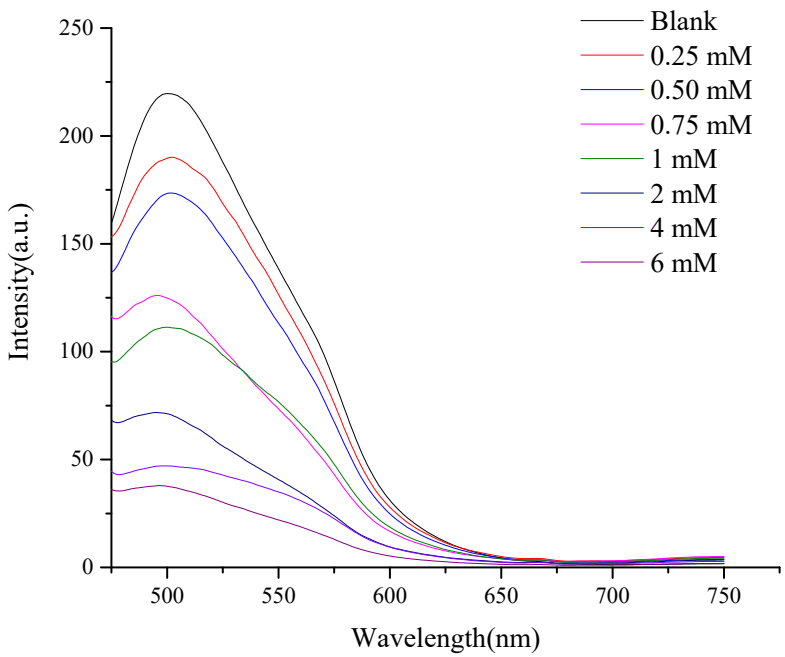

Fig. S39. PXRD patterns of complex **7** in Fe^{3+} solution for five cycles.

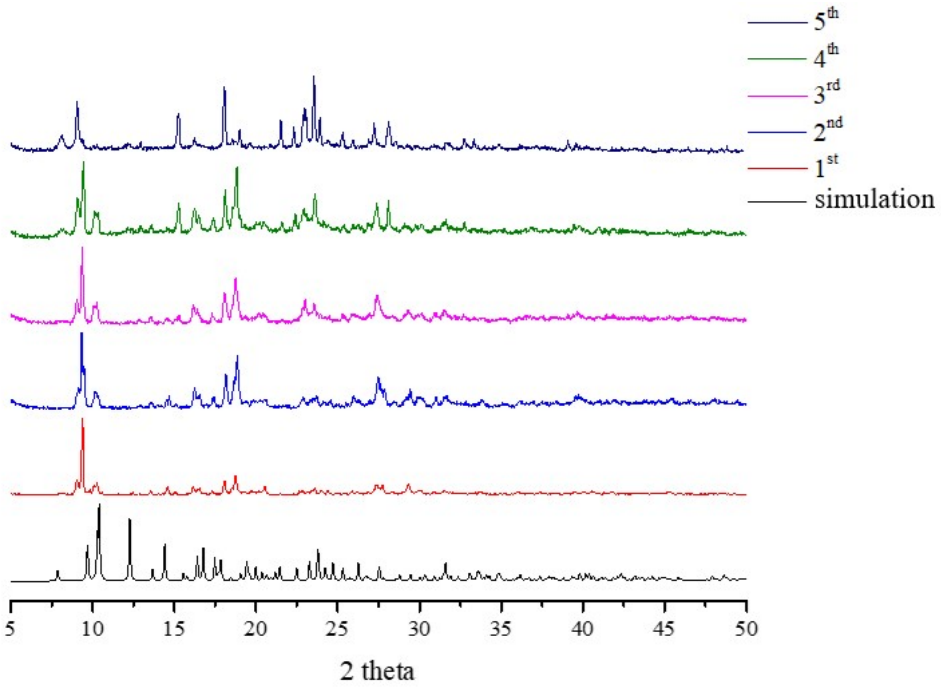

Fig. S40. N_2 adsorption−desorption isotherms for complex **1**.

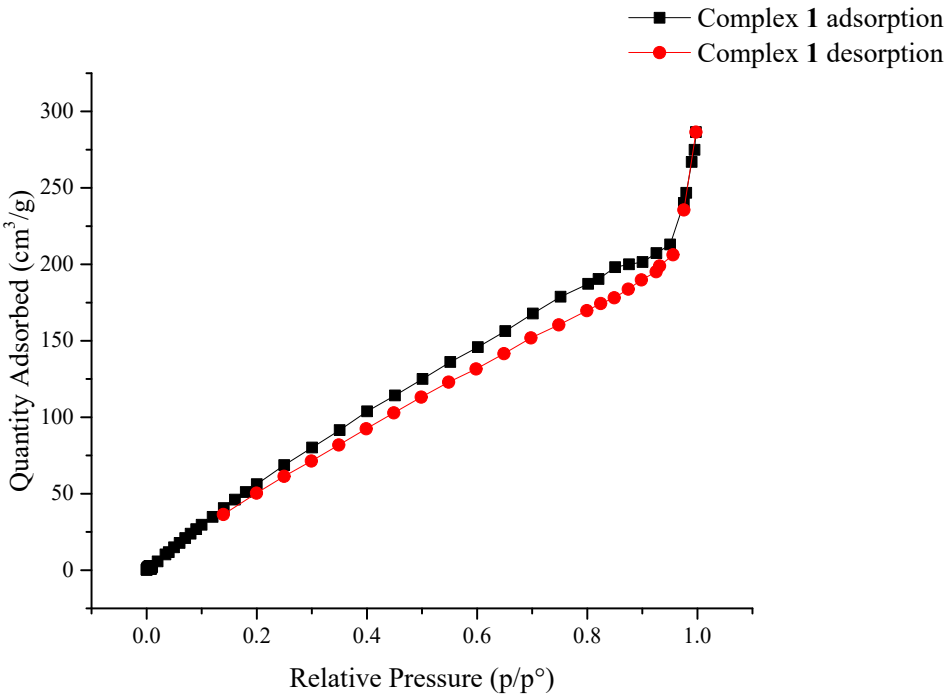

Fig. S41. Pore-size distribution curve for complex **1**.

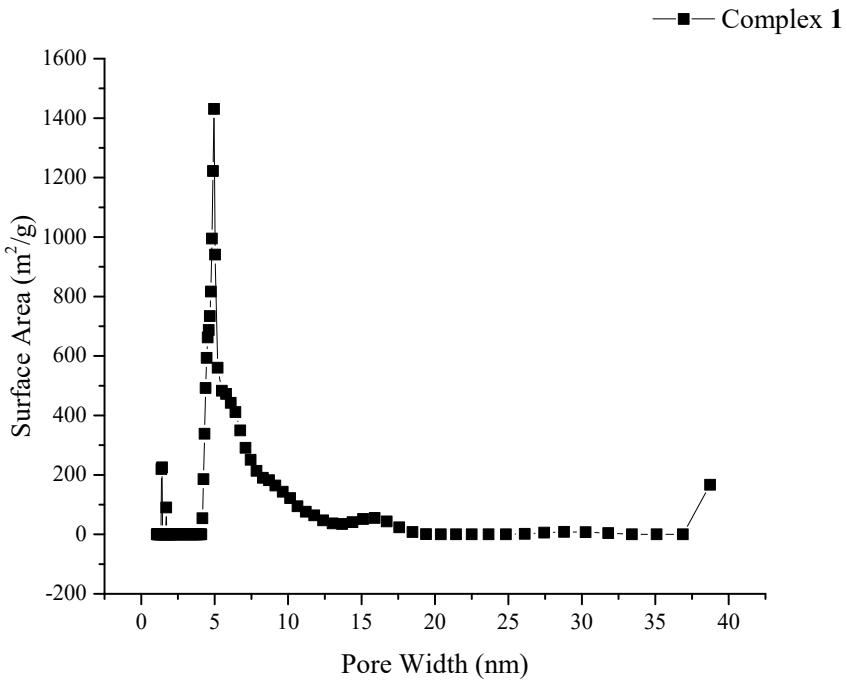

Fig. S42. N_2 adsorption−desorption isotherms for complex **2**.

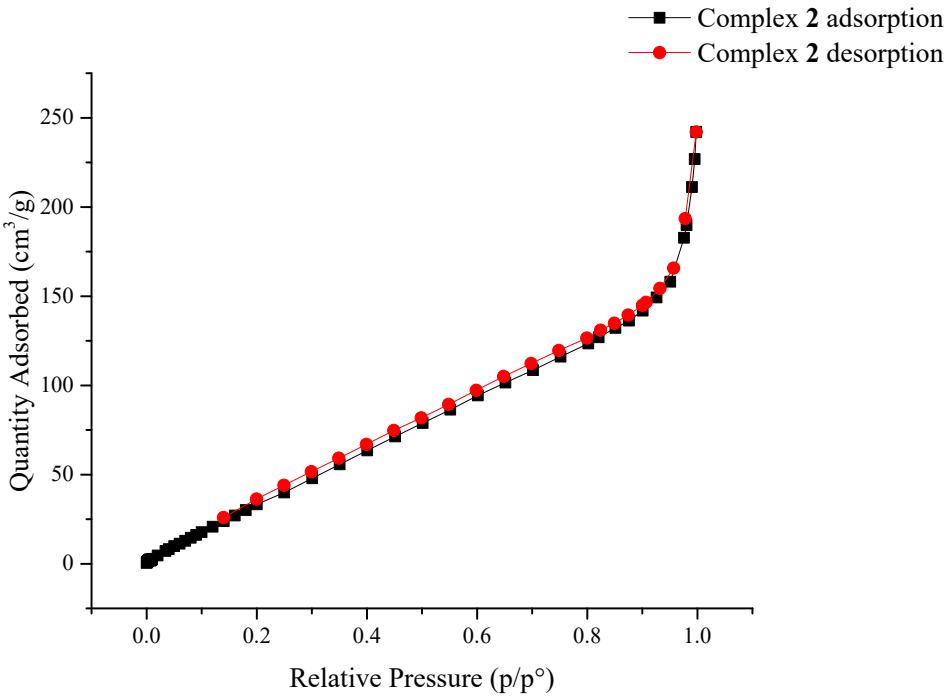

Fig. S43. Pore-size distribution curve for complex **2**.

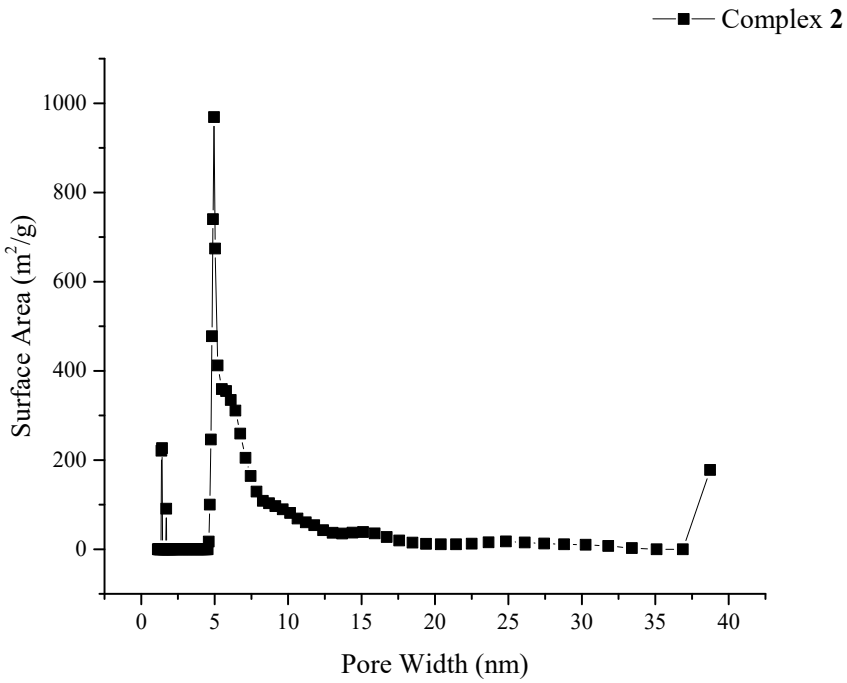

Fig. S44. N_2 adsorption−desorption isotherms for complex **3**.

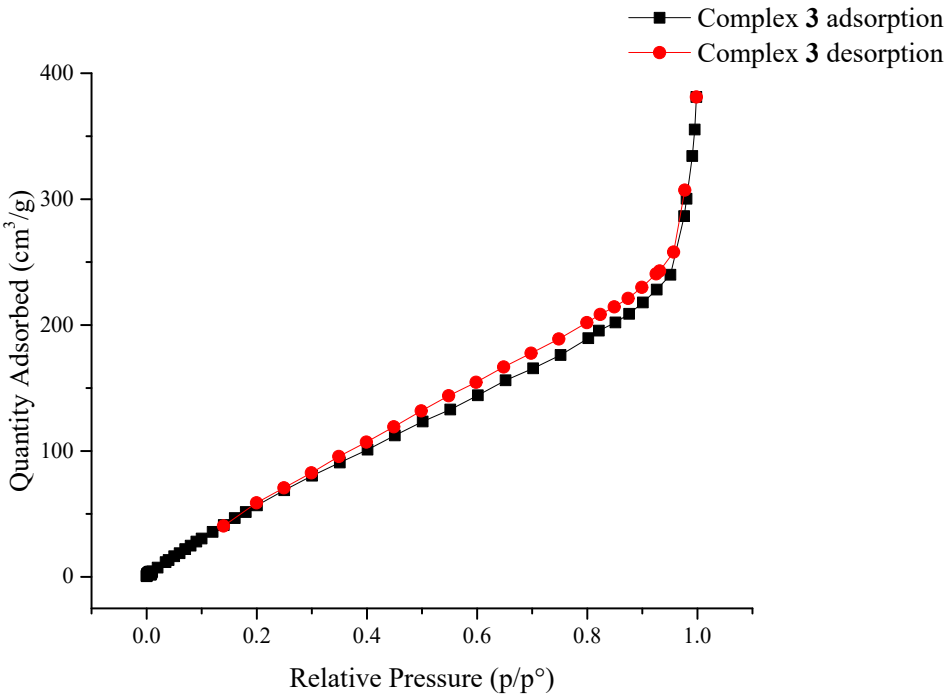

Fig. S45. Pore-size distribution curve for complex **3**.

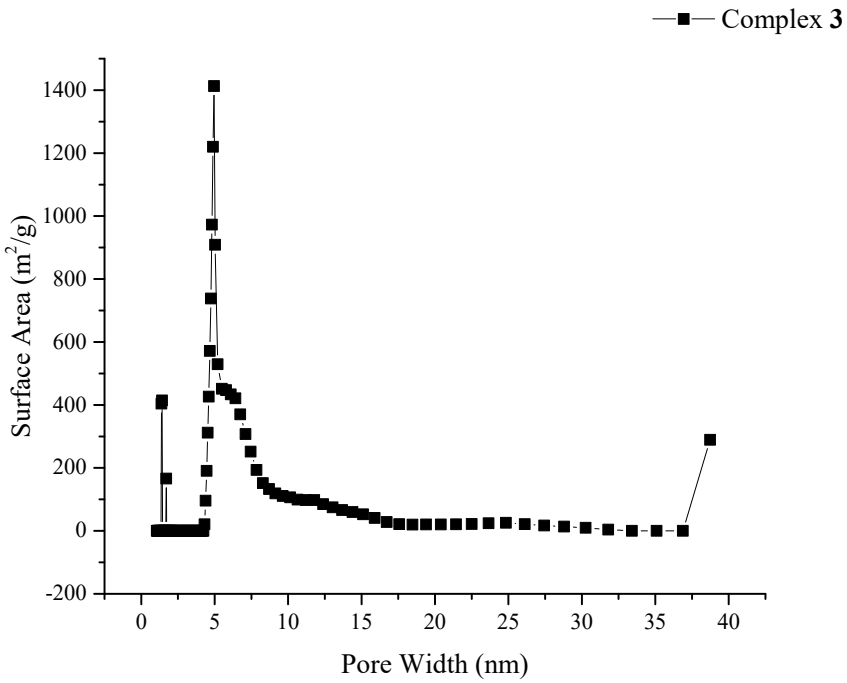

Fig. S46. N_2 adsorption−desorption isotherms for complex **6**.

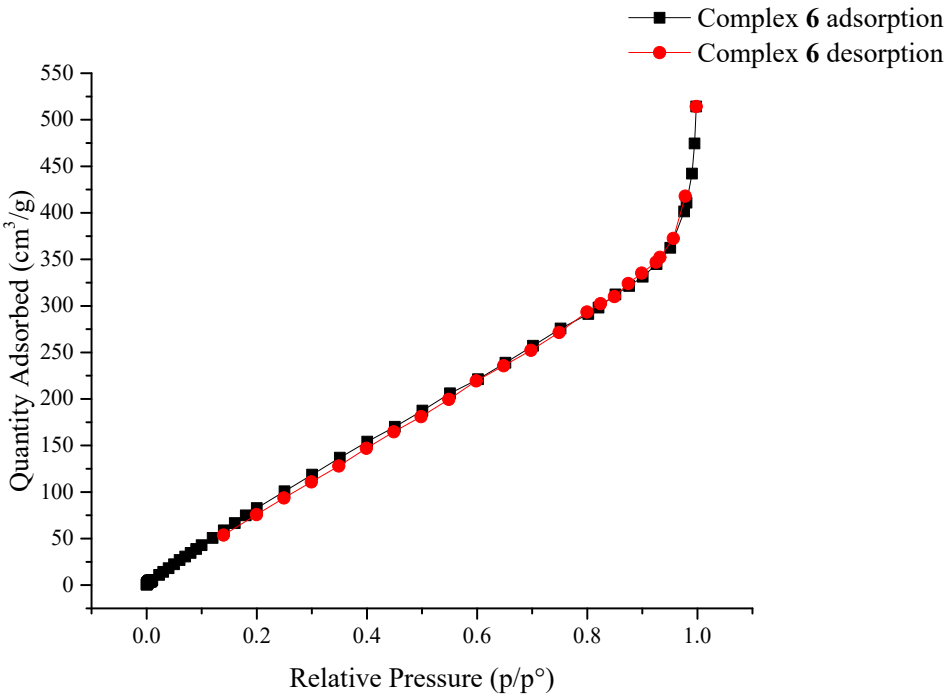

Fig. S47. Pore-size distribution curve for complex **6**.

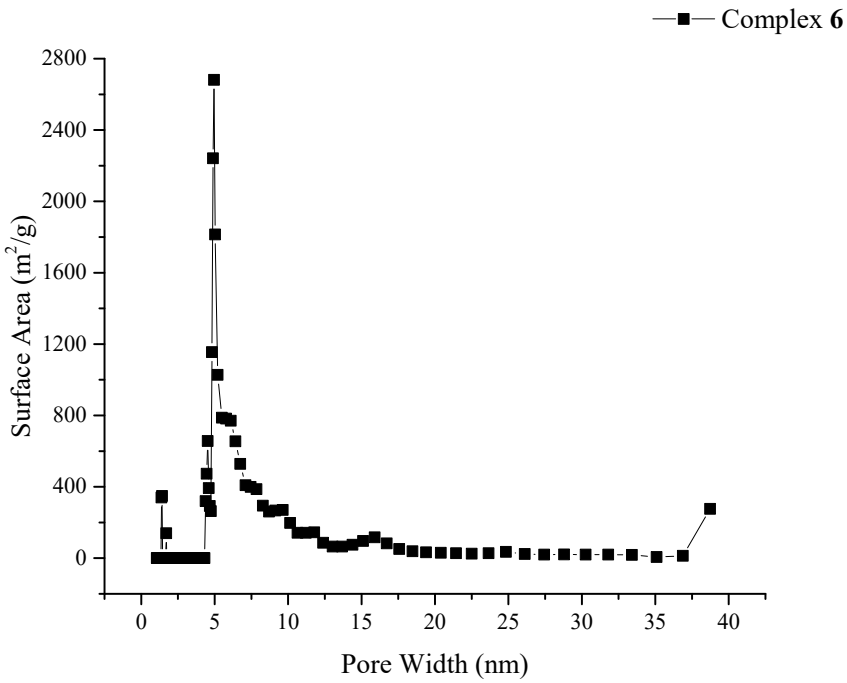

Fig. S48. N_2 adsorption−desorption isotherms for complex **7**.

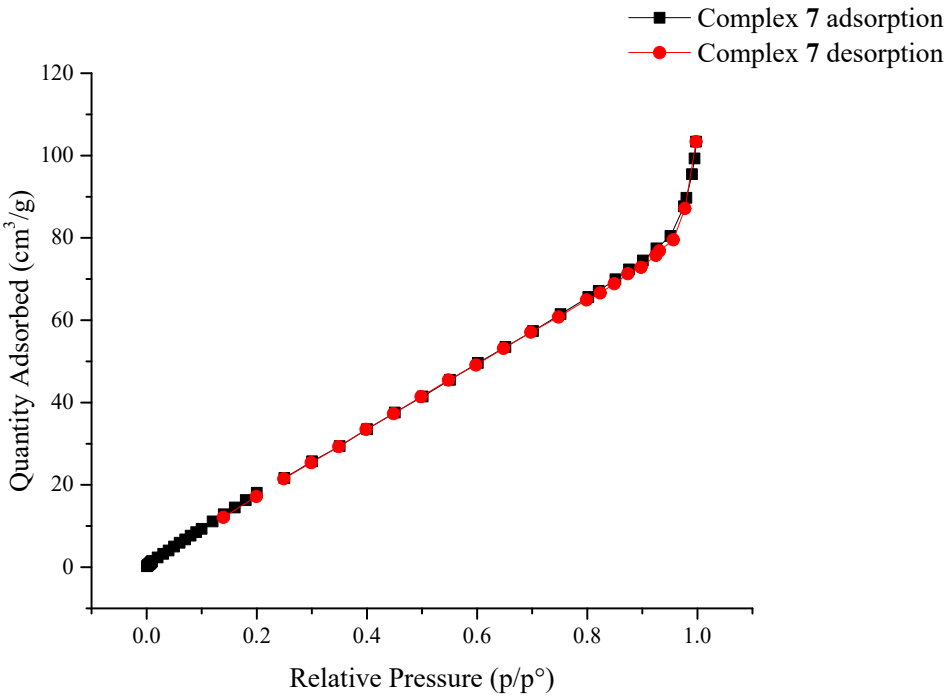

Fig. S49. Pore-size distribution curve for complex **7**.